Supporting Information

Polymer-confined synthesis of gram-scale high-entropy perovskite fluoride nanocubes for improved electrocatalytic reduction of nitrate to ammonia

Guohao Xue[a], Tianlu Wang[a], Hele Guo*[a,b], Nan Zhang[a], Claire J. Carmalt[c], Johan Hofkens[b], Feili Lai*[b,d] and Tianxi Liu*[a]

[a] The Key Laboratory of Synthetic and Biological Colloids, Ministry of Education, School of Chemical and Material Engineering, Jiangnan University, Wuxi 214122, P. R. China

[b] Department of Chemistry, KU Leuven, Celestijnenlaan 200F, Leuven 3001, Belgium

[c.] Department of Chemistry, University College London, London, WC1H 0AJ, UK

[d] State Key Laboratory of Metal Matrix Composites, School of Materials Science and Engineering, Shanghai Jiao Tong University, Shanghai 200240, P. R. China

* Corresponding authors (E-mails: hele.guo@kuleuven.be; feili.lai@kuleuven.be or feililai@sjtu.edu.cn; txliu@jiangnan.edu.cn)

Experimental Section

Materials

Anhydrous copper acetate ($CuAc_2$), magnesium acetate tetrahydrate ($MgAc_2{\cdot}4H_2O$), cobalt acetate tetrahydrate ($CoAc_2{\cdot}4H_2O$), zinc acetate dihydrate ($ZnAc_2{\cdot}2H_2O$), nickel acetate tetrahydrate ($NiAc_2{\cdot}4H_2O$), polyethylene pyrrolidone (PVP-K30), potassium fluoride dihydrate ($KF{\cdot}2H_2O$) were all purchased from Sinopharm Chemical Reagent Co., Ltd. Nafion solution (5 wt%) was provided by Adamas-beta Co., Ltd. The deionized (DI) water was produced by an ultrapure purification system. All chemicals were of analytical grade and used as received without further purification.

Materials characterization

The X-ray diffraction (XRD) patterns of samples were collected from a MiniFlex600 X-ray diffractometer with Cu Kα radiation (λ = 0.1542 nm) under a voltage of 40 kV and a current of 40 mA. The X-ray photoelectron spectroscopy (XPS) measurements and the valence band were performed on an Axis Supra by Kratos Analytical Inc. The carbon peak at 284.8 eV was used as a reference to correct the charging effects. Scanning electron microscopy (SEM) images were taken with a Hitachi S-4800 scanning electron microscope. Transmission electron microscopy (TEM) images and energy-dispersive X-ray spectroscopy (EDS) mappings were collected from a JEM-2100 plus transmission electron microscope by applying an acceleration voltage of 200 kV. Nuclear Magnetic Resonance (NMR) spectrum was collected from a JEOL JNM400S nuclear magnetic resonance spectrometer at 600 MHz resolution. The UV absorption spectra were collected from a WI 53711 ultra-microvolume spectrophotometer. The zeta potential measurement was performed using a Malvern Zetasizer Nano ZS90.

Electrochemical measurements

The electrochemical activity of HEPF-2 for NH_3 production was evaluated using an H-type electrolyzer and a CHI 660E electrochemical workstation in a standard three-electrode system. The pretreated Nafion 117 membrane (Dupont) was used as the separator, and 0.5 M K_2SO_4 electrolyte with or without 0.1 M KNO_3 was used in this experiment. Before tests, the Nafion 117 membrane was pretreated by heating it in H_2O_2 (5%) aqueous solution at 80 °C for 1 h and ultrapure water at 80 °C for another 1 h,

respectively, followed by treatment in 0.05 M H_2SO_4 for 1 h and ultrapure water for another 3 h. 6 mg of catalyst and 30 μL of 5% Nafion solution were dispersed in 470 μL ethanol by sonication to generate a homogeneous ink. Then, 25 μL catalyst ink was loaded onto a piece of carbon paper and dried naturally to obtain the working electrode. The geometric area of the working electrode was 1 × 1 cm^2, and the catalyst loading was around 0.3 mg cm^{-2}. The reference electrode was Ag/AgCl electrode (saturated with KCl solution), and the counter electrode was a carbon rod. All potentials were calibrated to a reversible hydrogen electrode (RHE) using the equation of $E_{RHE} = E_{Ag/AgCl} + 0.0591 \times pH + 0.197$.

Ammonia was determined using the spectrophotometric indophenol blue method with modifications involving dilution of post-test electrolytes to achieve the appropriate concentration for calibration curve matching. A 2 mL sample was taken from the electrochemical reaction vessel, followed by the addition of a solution containing 1 M NaOH, 5 wt% salicylic acid, and 5 wt% sodium citrate. Subsequently, 1 mL of 0.05 M NaClO and 0.2 mL of a 1 wt% aqueous solution of sodium nitroferricyanide ($C_5FeN_6Na_2O$) were added. After a 2-hour incubation at room temperature, the absorption spectrum was measured using an ultra-microvolume spectrophotometer to determine the formation of indophenol blue at 655 nm. The concentration–absorbance curves were calibrated using standard ammonia sulfate solutions, which contained the same concentrations of electrolytes as used in the electrocatalysis experiments.

The calculation method for yield rate of NH_3 and FE

The yield rate of NH_3 product and FE for NH_3 product were calculated at a given potential as follows:

$$\nu_{NH_3} = (c_{NH_3} \times V \times M) / (m \times t) \times 3600 \quad (1)$$

$$FE_{NH_3} = c_{NH_3} \times V \times N \times F / Q \quad (2)$$

where the ν_{NH_3} is the yield rate (mg h^{-1} $mg^{-1}_{cat.}$), c_{NH_3} is the measured NH_3 concentration (μmol mL^{-1}), V is the volume of the electrolyte (mL), M is the relative molecular mass of NH_3, which is 17 g mol^{-1}, m is the quality of the catalyst, t is the reduction reaction time (s), N is the number of electrons transferred for product formation, which is 8 for NH_3, F is Faraday constant, 96485.3 C mol^{-1}, Q is total electric charge (C).

Figures and Tables

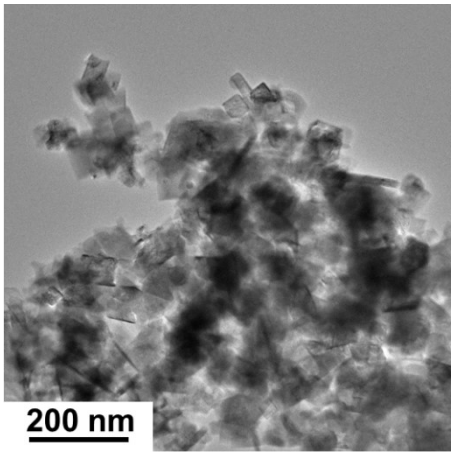

Fig. S1 The TEM image of HEPF-0.

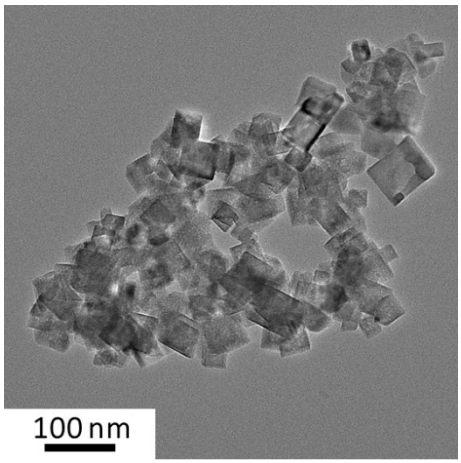

Fig. S2 The TEM image of HEPF-1.

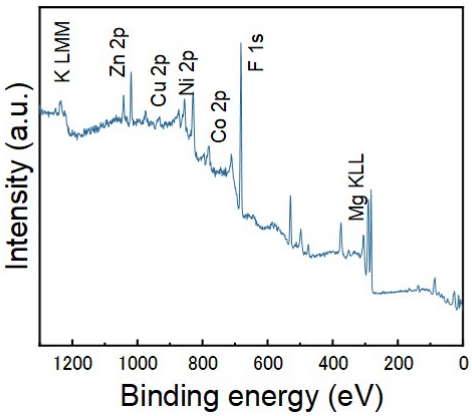

Fig. S3 The full XPS spectrum of HEPF-2.

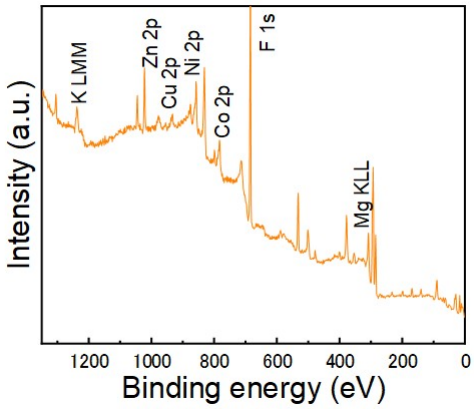

Fig. S4 The full XPS spectrum of HEPF-0.

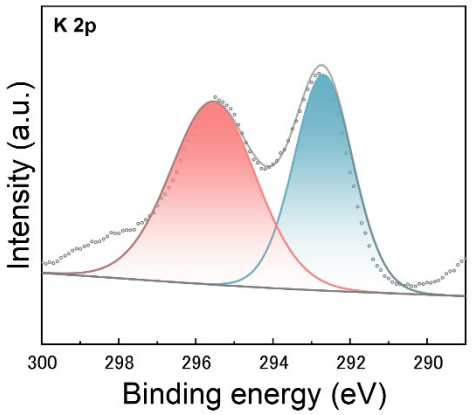

Fig. S5 High-resolution K 2p spectrum of HEPF-2.

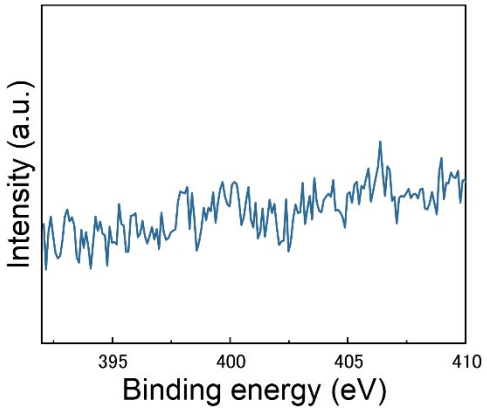

Fig. S6 High-resolution N 1s spectrum HEPF-2.

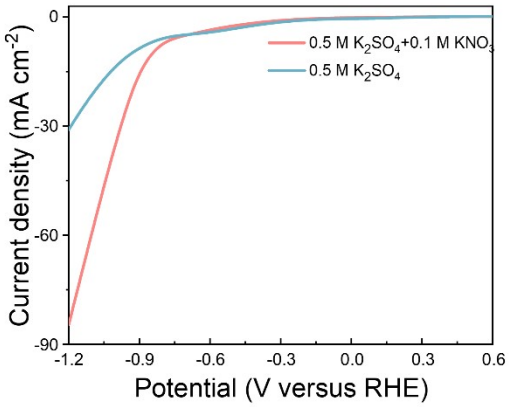

Fig. S7 LSV curves for HEPF-0 in 0.5 M K_2SO_4 electrolytes with and without KNO_3.

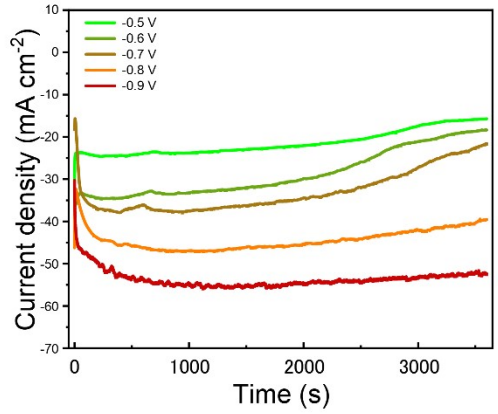

Fig. S8 Chrono-amperometry curves of the HEPF-2 at different potentials in 0.5 M K_2SO_4 electrolyte with 0.1 M KNO_3.

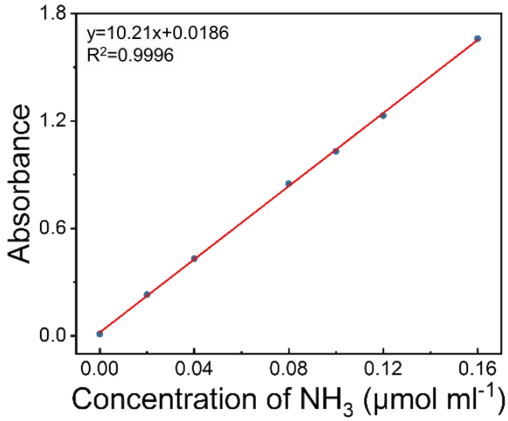

Fig. S9 The calibration curve for quantification of NH_3 indicates good linear relation of absorbance with NH_3 concentration ($y = 10.21x + 0.0186$, $R^2 = 0.9996$).

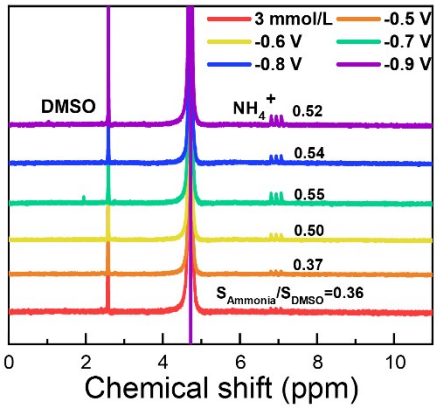

Fig. S10 ^{1}H NMR spectra of NH_4^+ under different potentials (V vs. RHE).

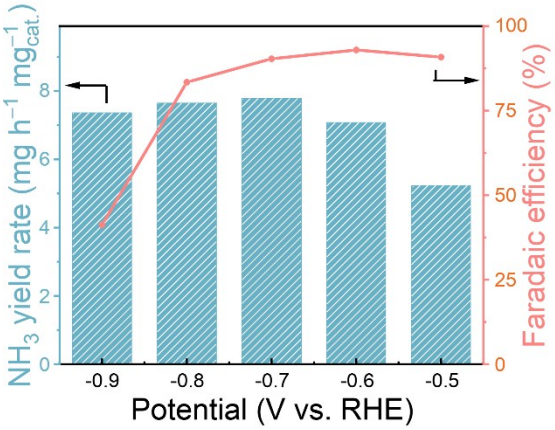

Fig. S11 NH_3 yield rates and FE values of HEPF-2 under different potentials by using NMR method.

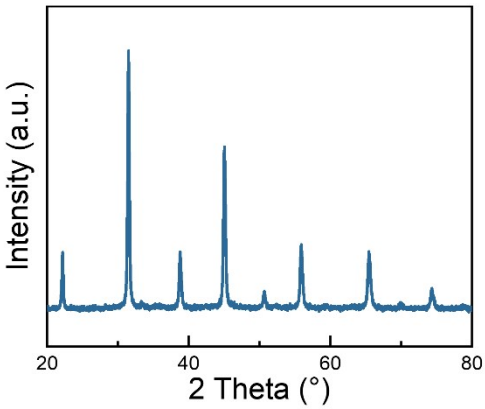

Fig. S12 XRD pattern of HEPF-2 after eNITRR.

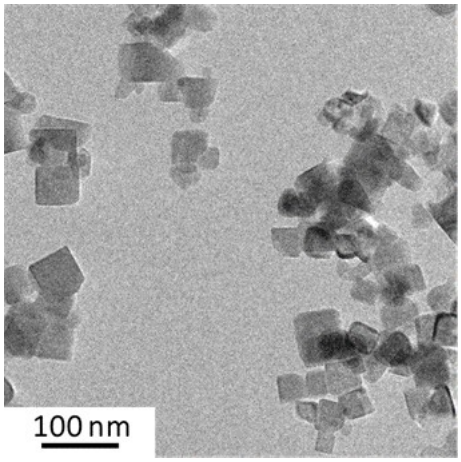

Fig. S13 TEM image of HEPF-2 after eNITRR.

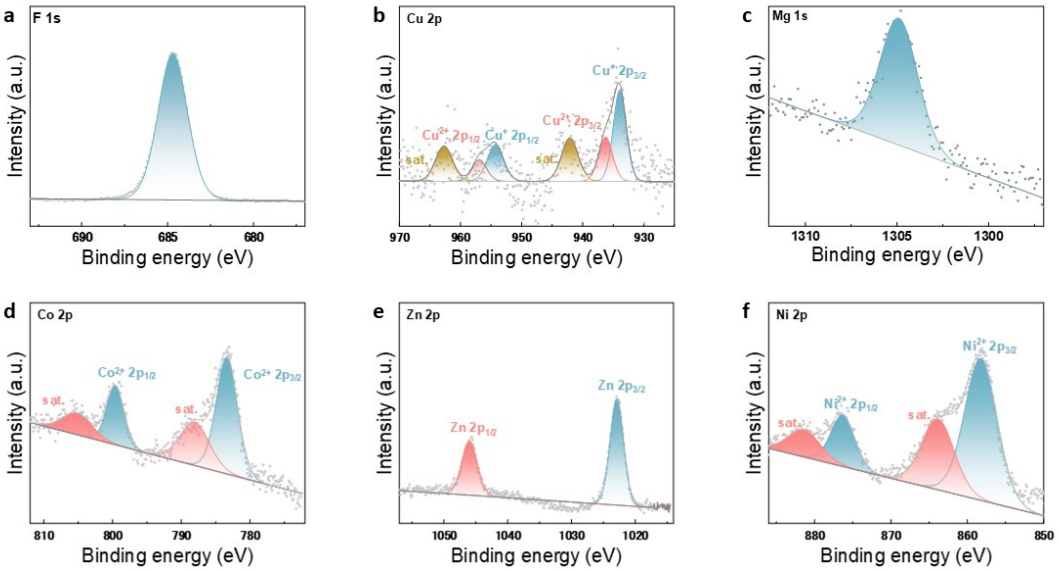

Fig. S14 High-resolution a) F 1s, b) Cu 2p, c) Mg 1s, d) Co 2p, e) Zn 2p, and f) Ni 2p XPS spectra HEPF-2 catalyst after eNITRR.

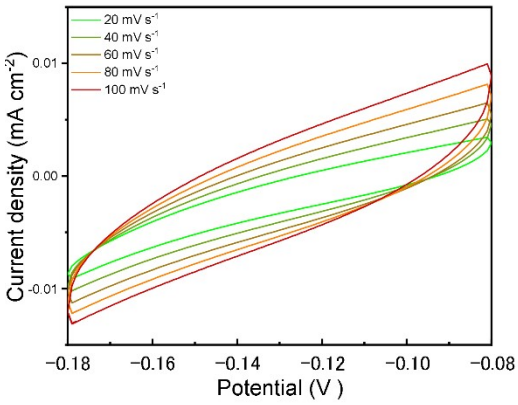

Fig. S15 CV curves of HEPF-2 at different scan rates from 20 to 100 mV s^{-1}.

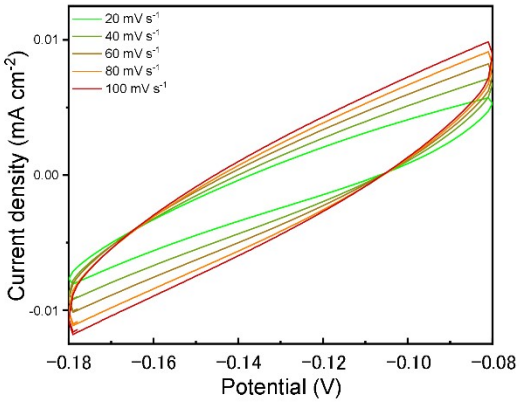

Fig. S16 CV curves of HEPF-0 at different scan rates from 20 to 100 mV s^{-1}.

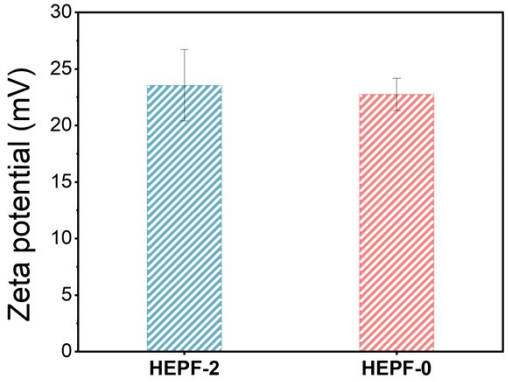

Fig. S17 Zeta potentials of HEPF-2 and HEPF-0.

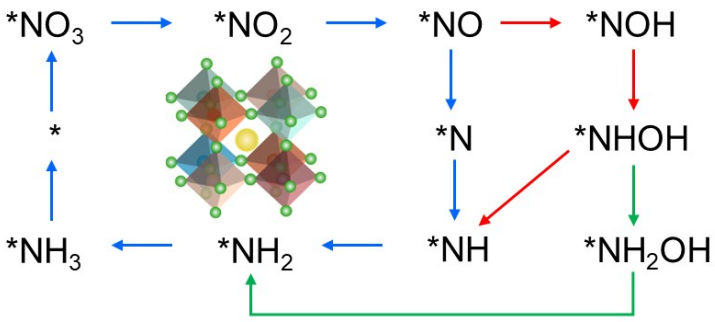

Fig. S18 Schematic diagram of possible pathways of eNITRR on HEPF.

Table S1 Comparison of the FE values and NH_3 yield rates of HEPF-2 with high-entropy catalysts reported in recent literature.

Catalyst	Electrolyte	FE (%)	NH_3 yield rate ($mg\ h^{-1}\ mg^{-1}_{cat.}$)	Ref.
LSNCMFC PNTs	0.5 M K_2SO_4 + 35.7 mM KNO_3	~100	1.66	1
Co-HEB	1 M KOH + 0.5 M NO_3^-	97.9	2.04	2
LMFCCZ	1 M KOH + 0.5 M NO_3^-	95.0	1.5	3
CuNiCoZnMn/CP	0.5 M Na_2SO_4 + 0.1 M KNO_3	96.62	12.3 mg h^{-1} cm^{-2}	4
Ru-MEA	0.5 M Na_2SO_4 + 50 mM $NaNO_3$	93.5	3.171 mg h^{-1} cm^{-2}	5
(FeCoNiCu)Ox/CeO_2	0.1 M KOH + 0.1 M KNO_3	90	30.3 mg h^{-1} cm^{-2}	6
RS-20	1 M KOH + 0.1 M KNO_3	93.4	4.84 mg h^{-1} cm^{-2}	7
CoFeNiO/$BiVO_4$	0.5 M Na_2SO_4 +150 ppm NO_3^-	30.3	0.01707	8
HEPF-2	0.5 M K_2SO_4 + 0.1 M KNO_3	92.8	7.03	This work

Reference

1. Y. Chen, C. Chen, W.-H. Huang, C.-W. Pao, C.-C. Chang, T. Mao, J. Wang, H. Fu, F. Lai, N. Zhang and T. Liu, *ACS Nano*, 2024, **18**, 20530-20540.
2. P. Chen, W. Zhong, Z. Gong, Q. Cao, H. Tang, Y. Chu and Y. Chen, *Catal. Today*, 2024, **439**, 114809.
3. L.-H. Yang, M.-T. Liao, Z.-Q. Lin, J.-X. Pan, W. Li, S.-H. Lv and H.-Y. Cheng, *Sep. Purif. Technol.*, 2024, **348**, 127781.
4. K. Zhang, Z. Zhang, T. Yang, S. Wang, S. Liu, Z. Zhao, S. Hu, Z. Ma, J. Huang, Y. Yang, Y. Chen and B. Ge, *ACS Appl. Mater. Interfaces*, 2024, **16**, 43526-43534.
5. M. Yang, B. Li, S. Li, Q. Dong, Z. Huang, S. Zheng, Y. Fang, G. Zhou, X. Chen, X. Zhu, T. Li, M. Chi, G. Wang, L. Hu and Z. J. Ren, *Nano Lett.*, 2023, **23**, 7733-7742.
6. Y. Qie, J. Gao, S. Li, M. Cui, X. Mao, X. Wang, B. Zhang, S. Chi, Y. Jia, Q.-H. Yang, C. Yang and Z. Weng, *Sci. China Mater.*, 2024, **67**, 2941-2948.
7. S. Sun, C. Dai, P. Zhao, S. Xi, Y. Ren, H. R. Tan, P. C. Lim, M. Lin, C. Diao, D. Zhang, C. Wu, A. Yu, J. C. J. Koh, W. Y. Lieu, D. H. L. Seng, L. Sun, Y. Li, T. L. Tan, J. Zhang, Z. J. Xu and Z. W. Seh, *Nat. Commun.*, 2024, **15**, 260.
8. F. Wang, Q. Ding, Y. Bai, H. Bai, S. Wang and W. Fan, *Inorg. Chem. Front.*, 2022, **9**, 805-813.